

C. N. E. A. Biblioteca	
ARCHIVO PUBLICACIONES	
Nº 1	AÑO 1979

01. 79. 09

The Stress Induced Phase Transformation in Martensitic Single Crystal of CuZnAl Alloys

Gabriel Barceló, Manfred Ahlers and Ricardo Rapacioli

(Centro Atómico Bariloche, Comisión Nacional de Energía Atómica, S.C. de Bariloche, R.N. - Argentina)



Sonderdruck aus Zeitschrift für Metallkunde
Band 70 (1979), H. 11, S. 732–738
DR. RIEDERER VERLAG GMBH STUTTGART

The Stress Induced Phase Transformation in Martensitic Single Crystal of CuZnAl Alloys

Gabriel Barceló, Manfred Ahlers and Ricardo Rapacioli

(Centro Atómico Bariloche, Comisión Nacional de Energía Atómica, S.C. de Bariloche, R.N. - Argentina)

The critical resolved shear stress for the transformation from martensite to fcc has been measured for ternary CuZnAl alloys. It is shown that the energy difference between the disordered fcc α phase solid solution and the ordered martensite at the same composition is the sum of an order contribution from fourth nearest neighbor pairs and of a term which is determined by the α phase stacking fault energy. Implications on martensitic transformations are discussed.

Spannungsinduzierte Phasenumwandlung in martensitischen Einkristallen von CuZnAl-Legierungen

Es wurde die kritische Schubspannung für die Umwandlung von Martensit zu einer flächenzentrierten Phase in Cu-Zn-Al-Legierungen gemessen. Es wird gezeigt, daß die Energiedifferenz zwischen dem ungeordneten α -Mischkristall (kfz) und dem geordneten Martensit aus zwei Anteilen besteht, einem Beitrag zur Fernordnung, der durch die Wechselwirkung viertnächster Nachbarpaare beschrieben werden kann, und einem Beitrag, der durch die Stapelfehlerenergie im α -Mischkristall bestimmt wird. Es werden Schlußfolgerungen bezüglich der Martensitumwandlung gezogen.

A martensitic CuZn single crystal can be produced by stressing in tension a single crystal of ordered bcc β phase of favorable orientation above the M_s temperature^{1) 2)}. With further stressing and beyond a critical value τ_B the martensitic single crystal itself gets deformed with the formation of a new phase having a different lattice^{1) 2)}. Surface observations have shown that this structural transformation is associated with a shear on the close packed (001) plane of the 3R orthorhombic martensite in the direction [100] (corresponding to a $\{111\}_{fcc} <112>_{fcc}$ system in a face centered lattice¹⁾). It has been concluded that the new phase is a long range ordered structure closer to fcc.

In binary CuZn the critical resolved shear stress τ_B is temperature independent but varies with the alloy composition¹⁾. On unloading the fcc phase persists in the binary CuZn alloys even below τ_B , and disappears only simultaneously with the retransformation to the β phase¹⁾, indicating that a hysteresis exists between the stress τ_B for the transformation to fcc and the stress τ_{ret} for the retransformation from fcc to martensite. If the hysteresis were absent τ_B would be a measure of the difference in free energy between the orthorhombic and the fcc long range ordered structures. It had been argued for CuZn²⁾ that although the hysteresis probably is not zero it is concentration independent, thus allowing to determine the concentration dependence of the free energy difference between the two phases.

The composition range in which martensitic single crystals can be obtained in binary CuZn is very limited, ranging from about 39.4 to 40.4 at. % Zn. More extensive variations in composition are, however, possible with ternary CuZn based alloys, that in addition provide the possibility to study the influence of electron concentration on martensite transformation temperature M_s .

Measurements of the critical stress have now been made in ternary CuZnAl alloys and are reported in this paper. As will be shown, the influence of long range order and of electron concentration can be separated and the con-

tribution from the hysteresis can be evaluated. The results are analysed in terms of a long range order contribution that can be described by fourth neighbor pair interaction energies and an electronic contribution that depends only on electron concentration.

Experimental Methods

Ternary Cu-Zn-Al alloys were prepared by melting 99.99% pure metals in sealed quartz tubes under an inert, argon atmosphere. Cylindrical β phase single crystals were grown subsequently, also in sealed quartz tubes by the Bridgman method. Two sets of alloys were prepared, one of constant electron concentration $e/a = 1.48$ with varying M_s temperature, and the other with a constant M_s of -50°C , but differing in e/a ratios. The M_s temperatures were obtained from electrical resistance measurements. Samples for tensile tests were prepared by spark machining the single crystals. The central part had a length of 20 mm and a diameter of 2.6 mm. At the ends the samples had shoulders that fitted into the grips of the tensile testing machine.

The orientations of the tensile axes as referred to the bcc lattice were determined by X-rays and are shown in fig. 1. Table 1 provides a list of the crystals with their compositions and the measured M_s . All samples were solution treated, to begin with, at 800°C and then air cooled. Quenching was avoided so as to eliminate quenched-in defects that otherwise have a strong influence on the transformation behavior of the alloy³⁾.

Martensite was stress-induced under tension, at a temperature above M_s in samples that had M_s above room temperature. Stress was applied until all material had transformed, which could be verified optically. The martensite single crystals so produced were cooled under constant stress to room temperature in order to retain them as such. These crystals were then deformed at room temperature until the new stress-induced phase appeared. The β phase crystals with M_s below room temperature, on the other hand, were continuously de-

formed under tension at temperatures above M_S at a deformation rate of 0.1 cm/min.

Results

A deformation cycle, starting with the β phase single crystals is shown in fig. 2. On loading the martensite is induced at a stress $\sigma_S^{\beta \rightarrow M}$ (load divided by initial cross section), and the transformation is complete at $\sigma_f^{\beta \rightarrow M}$. The stress then increases rapidly until at σ_B the martensite starts to deform, without marked hardening and associated with the appearance of deformation bands, very similar to those observed in binary CuZn¹⁾. On unloading the new phase starts to disappear at σ_{retr} but in general does not disappear completely, as the retransformation to the β phase occurs before at $\sigma_S^{M \rightarrow \beta}$. The curve in fig. 2 is altered, depending on the alloy composition: If σ_B is small or if $\sigma_S^{\beta \rightarrow M}$ is high at the deformation temperature used σ_{retr} may lie below $\sigma_S^{M \rightarrow \beta}$.

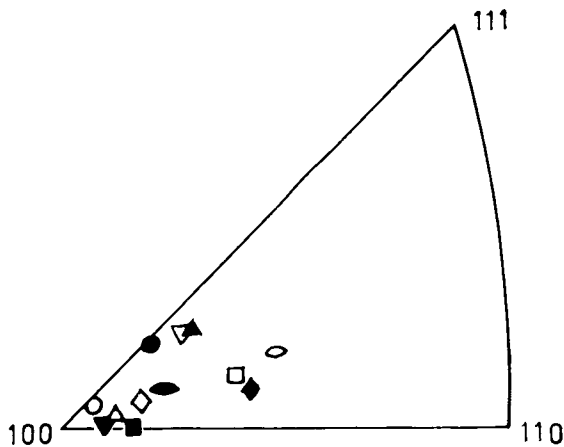


Fig. 1. Orientations of the tensile axes as referred to the bcc lattice. The symbols are the same as those in table 1.

The critical resolved shear stress τ_B on the relevant shear system was deduced from the measured σ_B , taking into account the orientation relationship between β and martensite, the change in orientation of the tensile axis during transformation and of the cross section of the induced martensite. The shear system that is activated at the stress σ_B in the ternary alloys is the secondary shear system $(001)_o, [100]_o$ of the orthorhombic martensite. This is supported, in addition to the results for CuZn¹⁾ by a crystallographic analysis of the surface markings in a ternary alloy with $M_S > 20^\circ\text{C}$, and by transmission electron microscopy to be discussed below.

The results of the measured critical stresses τ_B and τ_{retr} thus deduced are listed in the table and are plotted in fig. 3 to 5. The scatter in the data is partially caused by the serrations in the σ - ϵ curve near σ_B , that introduces some uncertainty in the determination of σ_B , and partially is al-

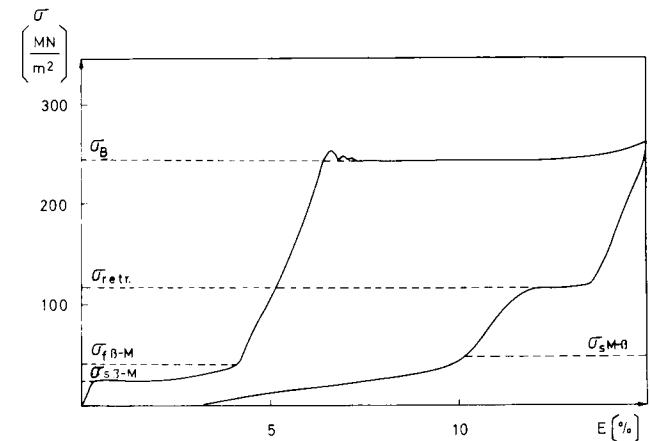


Fig. 2. A transformation cycle, stress σ versus strain ϵ . Other symbols explained in the text.

Sample	Alloy	Symb	Composition (at.%)			T.exp. °C	M _S °C	τ_{cr} MN/m ²	
			Cu	Zn	Al			τ_B	τ_{retr}
81	I	◆	63	26,7	10,3	-197	-250	194	
82p	II	▽	66,5	19	14,5	-65	-133	162	
82c	II	◀	II	II	II	-65	-133	147	
78p	III	■	69	14,4	16,6	17	-1	127	64
78c	III	■	II	II	II	17	-1	117	62
88c	IV	▲	70	12	18	17	62	114	61
49	IV	▽	II	II	II	20	74	120	
50	IV	●	II	II	II	20	77	127	
57c	V	◇	66,8	20,2	13	0	-45	113	66
57p	V	◇	II	II	II	-4	-45	117	56
48	V	◊	II	II	II	20	-53	116	
65p	VI	□	67,9	16,1	16	-27	-78	153	81
71	VI	▼	II	II	II	1	-69	146	77
59	VI	○	II	II	II	20	-42	155	
83c	VII	▽	68,9	12,1	19	-28	-44	161	95
51	VII	△	II	II	II	20	-32	178	

Table 1. The critical resolved shear stresses τ_{cr} for the beginning of the transformation to the stress induced new phase (τ_B) and for the start of the retransformation to martensite (τ_{retr}). T_{exp} the temperature of measurement. Samples with the same number have been cut from one single crystal, c denoting the lower part that solidified first, p the upper part. The orientations are shown in fig. 1, denoted by the same symbols Symb.

so due to small deviations of the nominal compositions which have a large effect on σ_B , as can be noted from figs. 4 and 5. This is supported by the scatter in M_S for the same nominal alloy composition (compare with the table).

In fig. 3 is shown the influence of the measuring temperature on τ_B , obtained from a sample with $M_S = -1^\circ\text{C}$ which has been subjected to loading-unloading cycles at various temperatures. After each cycle the sample has been reheated to 800°C , in order to eliminate any defect that is introduced during the cycle. The sequence in temperatures is $22^\circ\text{C}, -192^\circ\text{C}, +24^\circ\text{C}, -192^\circ\text{C}, +62^\circ\text{C}, +44^\circ\text{C}$.

Within experimental scatter the number of cycles does not affect τ_B . As can be noted from fig. 3 there is a small decrease in τ_B with decreasing deformation temperature. In comparison, the temperature dependence of τ_B for binary CuZn using the data of ref. 1) is smaller than that of the ternary alloy in fig. 3. At any rate the temperature dependence of τ_B is small compared to the composition dependence and therefore will be neglected in the analysis.

τ_B and τ_{retr} are drawn as a function of electron concentration in fig. 4 for the ternary alloys with a constant M_S temperature of about -50°C , and for the binary CuZn for which M_S varies with e/a ¹⁾. Extrapolation of both curves to $e/a = 1.382$ corresponds to the τ_B value for

the binary CuZn with an $M_S = -50^\circ\text{C}$. Both curves extrapolate to the same τ_B within experimental scatter, in spite of the fact that the ternary CuZnAl have DO_3 order and the CuZn only B2 order. This result indicates that for a given M_S the τ_B is only a function of the electron concentration. The retransformation stress lies 60 MN/m^2 below τ_B , with the same concentration dependence as τ_B .

In fig. 5 τ_B and τ_{retr} are plotted as a function of Al-concentration for a constant electron concentration. As can be seen, τ_B varies with composition even at a constant e/a , implying that e/a is not the only variable that controls τ_B .

The results of figs. 4 and 5 can be represented by the following equations:

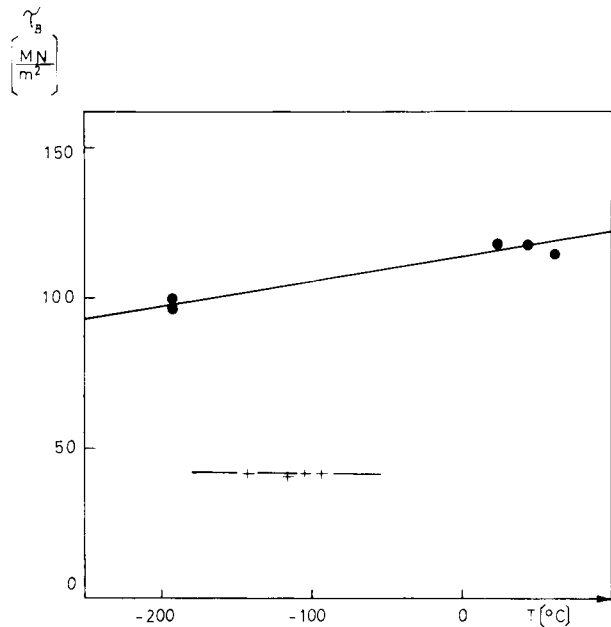


Fig. 3. Temperature dependence of the crss τ_B for Cu-14.4 at.% Zn-16.6 at.% Al (filled circles) and Cu-39.6 at.% Zn (crosses, from ref. 1)).

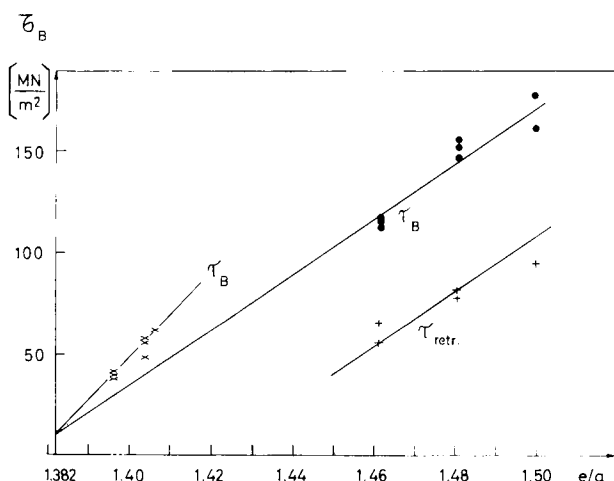


Fig. 4. Crss τ_B as a function of e/a at constant $M_S = -50^\circ\text{C}$ for ternary CuZnAl on transformation (filled circles) and on retransformation (crosses), and for binary CuZn (inclined crosses) on transformation (from ref. 1)).

(a) for $M_S = -50^\circ\text{C}$ in ternary CuZnAl:

$$\tau_B = -510 + 1.36 \cdot 10^3 (e/a - 1) [\text{MN/m}^2]$$

(b) for $e/a = 1.48$ in ternary CuZnAl:

$$\tau_B = 302 - 10^3 C_{\text{Al}} [\text{MN/m}^2]$$

(c) For binary CuZn:

$$\tau_B = -827 + 2.19 \cdot 10^3 C_{\text{Zn}} [\text{MN/m}^2]$$

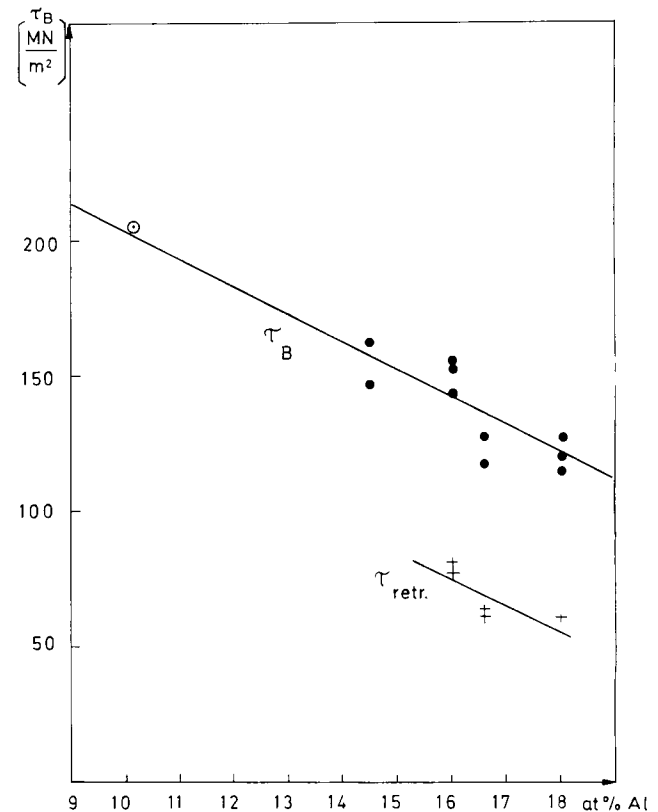


Fig. 5. Crss τ_B as a function of Al concentration at constant $e/a = 1.48$, for CuZnAl, on transformation (circles) and retransformation (crosses). The open circle is the value from sample 81 adjusted to $e/a = 1.48$ using fig. 4.

Electron microscopy studies were also made in order to confirm that the structure induced by deformation of the martensite indeed is an ordered face centered one. The new phase was retained in an alloy Cu-12 at.% Zn-18 at.% Al as follows. After inducing the new phase, the samples were kept for a week at 40°C without unloading. This procedure often leads to a stabilisation, whose origin is not clear. Thin foils could then be prepared from the sample for TEM. An electron diffraction pattern from a foil cut normal to the compact plane is shown in fig. 6. It is evident that the spots corresponding to martensite are absent and the pattern is of a face centered lattice. Strong streaking is observed in the pattern due to additional stacking faults. The amount of streaking and therefore the faulting was found to be different in different regions of the foil.

Discussion

The stability of the equilibrium phases in the Cu-Zn system is controlled by the electron concentration e/a and the long range order⁴). It seems appropriate therefore to attempt a description of the stability difference between

the 3R ordered orthorhombic martensite and the stress induced ordered fcc lattice in terms of two contributions, one that is independent of the atom distribution for a given composition, but depends on electron concentration, and the other which takes into account the ordering. The latter has been described with great success by pairwise interaction energies^{5) 6)}. This approach therefore will also be adopted in the present discussion. Further, the transformation from 3R to fcc by a shear on the

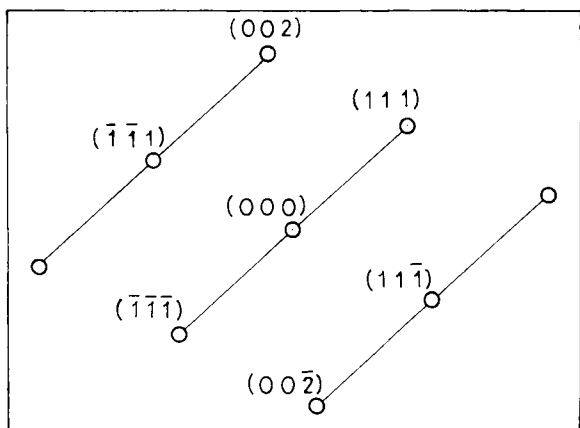


Fig. 6. TEM diffraction pattern and the schematic representation.

(001) [100] system does not change the order contributions from first and second neighbors, only the third and higher order neighbors are affected.

The energy difference between 3R and fcc resulting from the order can be calculated by counting the number of bonds for a given neighbor pair and multiplying them with the corresponding pair interaction energies. This has been done in a previous paper⁷⁾ for the alloys which have the B2 long range ordered structure in the high temperature β phase. It will be extended now to the DO₃ ordered structure, which is present in the alloys studied here. The following definitions are used:

Let $M_{AB}^{(i)}$ be the interaction energy between an atom A and B (A, B = Cu, Zn, Al) in i -th neighbor position. Then a "chemical interaction energy" $m_{AB}^{(i)}$ can be defined by $m_{AB}^{(i)} \equiv -2M_{AB}^{(i)} + M_{AA}^{(i)} + M_{BB}^{(i)}$, where $A \neq B$. The long range order in the 3R martensite is that inherited from the high temperature β phase, since the martensitic transformation is a diffusionless one. It is sufficient therefore to characterize the order in 3R by the order in DO₃, which is usually described by subdividing the lattice into four parallel fcc sublattices with lattice constant $2a$,

the origin of the sublattice I, II, III and IV given by (0, 0, 0), (a, 0, 0), $a(1/2, 1/2, 1/2)$ and $a(1/2, 1/2, -1/2)$ respectively. The occupation probability of having an A atom on any site of sublattice $J = I$ to IV is ρ_A^J , with $\rho_A^I + \rho_B^I + \rho_C^I = 1$ for a ternary alloy. It is convenient to introduce the parameters $x_A \equiv (\rho_A^I + \rho_A^{II} - \rho_A^{IV})$; $y_A = 1/2(\rho_A^I - \rho_A^{II})$ and $z_A = 1/2(\rho_A^{III} - \rho_A^{IV})$. For B2 order $x_A \neq 0, y_A + z_A = 0$ and for DO₃ order $x_A \neq 0, y_A = 0, z_A \neq 0$.

Interactions up to eighth neighbors in the 3R structure have been included in the present evaluation of the energy difference between 3R and fcc. Below ninth neighbors the pairs do not extend across more than three neighboring close packed planes, the ninth neighbor distance corresponding to a $\langle 111 \rangle$ in a fcc lattice, the first to extend across four close packed planes. Therefore to eighth neighbors the difference in ordering energy between 3R and fcc is the same as 2/3 of that between hexagonal and fcc. The energy difference between fcc and 3R can be written as

$$E^{fcc} - E^M = \Delta (E_{el}^{fcc} - E_{el}^M) - \sum_{A, B} \Delta^{(1)} E_{AB}^{fcc-M} \cdot (C_A C_B + x_A x_B) - \sum_{A, B} \Delta^{(2)} E_{AB}^{fcc-M} (C_A C_B - x_A x_B) - \sum_{A, B} \Delta^{(3)} E_{AB}^{fcc-M} z_A z_B$$

The sum extends over all different pairs. The first term on the right describes the part that is insensitive to the atom distribution but depends on the electron concentration e/a . For the alloy compositions considered in the present paper, $\Delta (E_{el}^{fcc} - E_{el}^M)$ will be approximated by a linear function of e/a .

$\Delta^{(1)} E_{AB}^{fcc-M}$ and $\Delta^{(2)} E_{AB}^{fcc-M}$ have been derived earlier⁷⁾ and are given by

$$\Delta^{(1)} E_{AB}^{fcc-M} = \frac{2N}{3} (-m_{AB}^{(3)} + m_{AB}^{(4)} - 2m_{AB}^{(5)} + 3m_{AB}^{(6)} + 2m_{AB}^{(7)} - 2m_{AB}^{(8)})$$

$$\Delta^{(2)} E_{AB}^{fcc-M} = \frac{2N}{3} (2m_{AB}^{(4)} - 4m_{AB}^{(5)} + 4m_{AB}^{(7)} - 4m_{AB}^{(8)})$$

In addition we have here the term which has to be considered for DO₃ order with $z \neq 0$:

$$\Delta^{(3)} E_{AB}^{fcc-M} = \frac{N}{3} (-m_{AB}^{(3)} + m_{AB}^{(4)} + 2m_{AB}^{(5)} - m_{AB}^{(6)} - 2m_{AB}^{(7)} - 2m_{AB}^{(8)})$$

where N is the number of atoms.

The following remarks concerning the equations will now be made:

a) Chemical pair interaction energies had been deduced from X-ray measurements in several short range ordered alloy systems and it had been shown that they oscillate with decreasing amplitude at increasing pair distance⁸⁾. Such a behavior has been explained by the incomplete shielding of extra charges by the conduction electrons⁹⁾. In the free electron approximation the chemical interaction energy $m_{AB}^{(i)}$ for atom pairs sufficiently far apart is given by $m_{AB}^{(i)} = \phi_{AB} (\cos (2k_F \cdot r_i + \varphi_{AB}) / r_i^3)$ where ϕ_{AB} and φ_{AB} are constants, r_i the distance between an atom pair i and k_F the wave vector at the Fermi surface for free electrons. The k_F and consequently $m_{AB}^{(i)}$ depends on the electron concentration. For fourth nearest neighbors

with distance $r_4 = (\sqrt{6/2}) a_{\text{fcc}}$ a change of electron concentration from $e/a = 1.382$ to 1.48 corresponds to a change in $2k_F \cdot r_4$ by 17.8%. This change is too large to be neglected, and therefore an e/a dependence of $m_{\text{AB}}^{(i)}$ (and consequently of $\Delta^{(2)} E_{\text{AB}}^{\text{fcc-M}}$) has to be taken into account in the following discussion.

b) Since the fifth, seventh and eighth nearest neighbor distances ($1.354 a_{\text{fcc}}$, $1.581 a_{\text{fcc}}$ and $1.683 a_{\text{fcc}}$) are appreciably larger than fourth neighbor distances ($1.225 a_{\text{fcc}}$) the $m^{(i)}$, $i > 4$ will be neglected in the following, and the corresponding terms in $\Delta^{(i)} E_{\text{AB}}^{\text{fcc-M}}$ as well, since their multiplicity remains small.

c) It is seen that in $\Delta^{(1)} E_{\text{AB}}^{\text{fcc-M}}$ and $\Delta^{(3)} E_{\text{AB}}^{\text{fcc-M}}$ the differences $m_{\text{AB}}^{(3)} - m_{\text{AB}}^{(4)}$ enter as leading terms. The $m_{\text{AB}}^{(3)}$ and $m_{\text{AB}}^{(4)}$ correspond to pairs which differ only by 6% in their distance⁷⁾, suggesting that $m_{\text{AB}}^{(3)} \approx m_{\text{AB}}^{(4)}$. This assertion is supported by the results discussed in fig. 4 which have shown that an extrapolation of τ_B from the DO₃ and B2 alloys yields the same value, implying that the $\Delta^{(3)} E_{\text{AB}}^{\text{fcc-M}}$ terms which describe second neighbor order can be neglected. The difference $m_{\text{AB}}^{(3)} - m_{\text{AB}}^{(4)}$ appears also in $\Delta^{(11)} E_{\text{AB}}^{\text{fcc-M}}$, which therefore will be neglected too.

d) For the ternary CuZnAl alloys the three chemical interaction energies $m_{\text{CuZn}}^{(4)}$, $m_{\text{CuAl}}^{(4)}$ and $m_{\text{AlZn}}^{(4)}$ have to be evaluated. The $m_{\text{AlZn}}^{(4)}$ can safely be assumed to be zero, since first and second neighbor chemical interaction energies in the β phase are also negligible for Al-Zn pairs¹⁰⁾. The ratio $f \equiv m_{\text{CuAl}}^{(4)}/m_{\text{CuZn}}^{(4)}$ can be deduced in the following way: the long range order in the 3R martensite causes a small lattice distortion¹¹⁾. This distortion depends on composition and is related to the M_s temperature¹²⁾. Since the M_s temperature is determined mainly by $m_{\text{AB}}^{(4)}$, it is possible to deduce f from the effect that a third element has on M_s , i.e. one Al atom has to be replaced by f Zn atoms in order not to change M_s . The M_s temperatures for CuZnAl with small amounts of Al and B2 order have been measured¹³⁾. It follows from this data that $f = 1.375$. The same f also fits the results for M_s of CuZnAl alloy with higher Al content and DO₃ order. We shall therefore substitute in the following for $m_{\text{CuAl}}^{(4)} = fm_{\text{CuZn}}^{(4)}$.

e) The energy difference $E^{\text{fcc}} - E^{\text{M}}$ can equivalently be expressed in terms of stacking fault energy Γ considering the 3R lattice as a basic fcc ordered structure with a regular array of stacking faults. The order contribution per stacking fault within the approximation to eighth neighbors (i.e. interaction between three neighboring close packed planes only) is independent of the density and distribution of the stacking faults. The same is not necessarily true for that electronic contribution which is insensitive to order. The partial dislocation which trails behind a stacking fault starts to move under a critical stress τ given by $\Gamma = \tau b_p$, where b_p is the Burgers vector of the partial dislocation. If a long or short range friction stress τ_{fr} is present, then τ is the difference between the applied τ_B and the friction stress τ_{fr} . Since the stress τ_B (fig. 3) does not increase with decreasing temperature, short range obstacles that can be overcome by thermally activated processes can be of no importance. The observed hysteresis during a loading and unloading cycle (fig. 2) permits to give an upper limit for the friction stress as 60 MN/m^2 . It is likely that the friction stress is considerably lower than this value. If the friction is due to the solid solution hardened lattice, then its stress should be independent of the direction in which the partial moves, and have a value given by $\tau_{\text{fr}} = 1/2 \cdot 60 \text{ MN/m}^2$. If the dislocation density increases with the deformation, then the retransformation on unloading should require an even

larger reverse stress, leading to a friction stress on transformation of $\tau_{\text{fr}} < 30 \text{ MN/m}^2$. A third estimate of τ_{fr} can be based on an extrapolation of the plateau stress in the disordered α phase CuZn to $e/a = 1.48$ assuming that long range order does not increase this stress. In this manner another upper limit value¹⁴⁾ for τ_{fr} can be derived. Using $d\tau_B/dC_{\text{Zn}}^{2/3} = 41 \text{ MN/m}^2$ and taking into account the smaller Burgers vector of the partial dislocation compared to a $a/2\langle 110 \rangle$ we get for $\tau_{\text{fr}} \leq 15 \text{ MN/m}^2$.

f) In the present alloys the investigations were carried out at temperatures considerably below the order-disorder temperatures, hence it can be assumed that maximum possible long range order is already reached, which implies that $C_A C_B - x_A x_B = C_B$ for $A = \text{Cu}$, $B = \text{Zn}$, Al . It is now possible to write the transformation enthalpy, taking into account the simplifications made so far, by:

$$E^{\text{fcc}} - E^{\text{M}} = \Delta (E_{\text{el}}^{\text{fcc}} - E_{\text{el}}^{\text{M}}) - \frac{4}{3} N m_{\text{CuZn}}^{(4)} (C_{\text{Zn}} + f C_{\text{Al}})$$

where $\Delta (E_{\text{el}}^{\text{fcc}} - E_{\text{el}}^{\text{M}}) = \Delta E_{\text{el}}^{\circ} (e/a - 1)$.

Using this equation, $m_{\text{CuZn}}^{(4)}$ at constant $e/a = 1.48$ can be calculated from the slope of the line in fig. 5 as $m_{\text{CuZn}}^{(4)}(1.48) = -260 \text{ [K]}$ (The $m_{\text{CuZn}}^{(i)}$ are expressed in units of the Boltzmann constant and have the dimension of K). In addition, $m_{\text{CuZn}}^{(4)}$ for an electron concentration near $e/a = 1.40$ can be determined from fig. 4. The line for the ternary alloys describes the influence of e/a on τ at a constant M_s , the difference to that for the binary CuZn thus comes from the change in M_s , and amounts to $-4/3 m_{\text{CuZn}}^{(4)} (0.382 - C_{\text{Zn}})$ in energy, from which a value $m_{\text{CuZn}}^{(4)} = -110 \text{ [K]}$ is calculated for $e/a = 1.40$. From these experimentally determined $m_{\text{CuZn}}^{(4)}$ several conclusions can be drawn, which will now be discussed in detail.

1) The values of $m_{\text{CuZn}}^{(4)}$ depend on composition, a behavior that is already expected from the composition dependence of k_F , as discussed earlier, but may also be due to a composition dependence of ϕ_{CuZn} and φ_{CuZn} . Since no further information is available at this moment on how $m_{\text{CuZn}}^{(4)}$ depends on composition, this point will not be pursued in this paper.

2) The $m_{\text{CuZn}}^{(4)}$ for $e/a = 1.382$ is in close agreement with a value which has been deduced from independent experiments: it had been shown that the concentration dependence of the transformation temperature M_s between β and martensite is essentially determined by $m_{\text{AB}}^{(4)}$, under the hypothesis that the $m_{\text{AB}}^{(i)}$ are structure insensitive, in the sense that they only depend on the i -th neighbor distance and not whether the lattice is fcc or bcc. The value that had been deduced was $m_{\text{CuZn}}^{(4)} = -125 \text{ [K]}^7)$, in very close agreement with the present results, supporting further the approach used to describe order effects by pairwise chemical interaction energies.

3) By subtracting the long range order contribution from the measured energy differences $E^{\text{fcc}} - E^{\text{M}}$ (more precisely the τ_B), the values for the disordered lattice should be obtained. This evaluation has been done for Cu-0.396 Zn and for Cu-0.48 Zn, the latter by extrapolating to $C_{\text{Al}} = 0$ from the ternary alloys at $e/a = 1.48$ (fig. 5). The extrapolation introduces some uncertainties due to the large concentration range used for extrapolation. Figure 7 shows the results. In order to compare with the other curves to be discussed subsequently, it is convenient to consider the 3R structure as an fcc lattice with stacking faults and to calculate the difference between the disordered 3R and fcc structure per stacking fault, which is denoted by a square associated with a bar. The square

corresponds to a zero friction stress of the moving partials, whereas the bar indicates the range of uncertainty if a friction stress up to one half of the hysteresis stress is admitted. As has been discussed earlier, it is likely that the friction stress is considerably smaller than half the hysteresis stress, and therefore the correct value is expected to be close to the square. In the same figure is also shown the energy difference per stacking fault between the ordered fcc and 3R, denoted by Γ . The two lines correspond to a zero friction stress and to a friction stress that is one half of the hysteresis stress. Furthermore, in the same figure are also shown stacking fault energies γ of the disordered α phase solid solution of CuZn, according to node measurements by various authors^{15) 16)}. The α -phase γ values have been extrapolated (the continuous curve at $\gamma > 0$), using a linear relationship between $\log \gamma$ and $[c/(c + 1)]^2$, where $c = 3(e/a - 1)$ ¹⁶⁾. This empirical relationship describes very well the behavior of various binary Cu alloys over a large concentration range¹⁶⁾. The agreement between the extrapolated γ values from α phase and the data deduced from the martensite at small friction stresses is excellent. This means that (within experimental uncertainty) the disordered 3R structure can be considered as a basic fcc disordered α phase with a stacking fault density 1/3. This result implies that the regularity of the stacking fault distribution in 3R does not constitute any important element of phase stabilization.

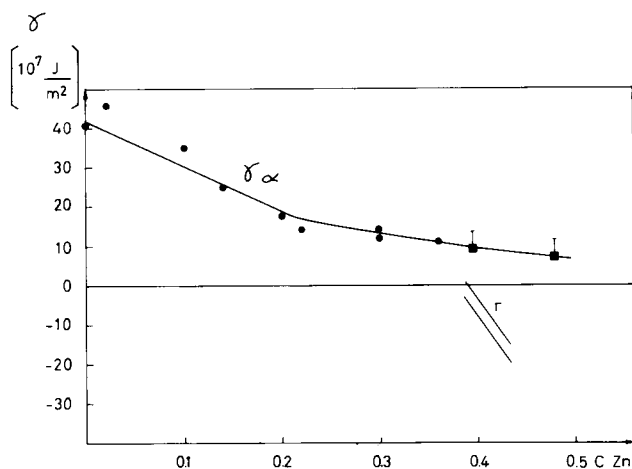


Fig. 7. Stacking fault energies SFE as a function of zinc concentration in binary CuZn: Filled circles: SFE of α phase. Lines denoted by Γ : Range of SFE for the ordered 3R martensite. Filled square: calculated SFE for disordered 3R, the bar indicates the uncertainty range (see text).

Thus the martensitic long range ordered 3R, which is obtained by a diffusionless transformation from β can be related in a simple way to the disordered fcc α phase which is stable at lower zinc concentration. Its energy consists of three components: The energy of the α phase CuZn alloy (at the corresponding composition), second the energy contribution from the stacking faults, characterized by the stacking fault energy γ , and third the order contribution using the fourth neighbor chemical interaction energy $m_{\text{CuZn}}^{(4)}$.

The entropy difference ΔS between the α phase and the ordered martensite is small. This can be seen by splitting ΔS into a contribution due to the phase change between α phase disordered and ordered fcc, and a contribution between ordered fcc and ordered 3R. The first term has been shown to be small⁷⁾, and the second remains also

small, since the temperature dependence of the critical resolved shear stress is quite temperature insensitive. Such a behavior is also expected from the small temperature dependence of the stacking fault energy in the α phase¹⁷⁾. It is therefore concluded that the entropy of formation of the 3R martensite is approximately the same as that of disordered α .

On the basis of the present discussion the stability of the 3R martensite can be compared with a hypothetical ordered fcc and hex martensite. The three structures differ in their stacking fault densities, and since their energies are linear functions of the fault density, the most stable of the three lattices is either fcc (for $\Gamma > 0$) or hex (for $\Gamma < 0$). For $\Gamma < 0$ therefore, as in our CuZn alloys, a hexagonal martensite instead of a 3R martensite would be expected in striking contrast to the observations. The conclusions that can be drawn from this discrepancy is that 3R forms, not because of its higher thermodynamic stability, but due to the very restricted transformation mechanism involved, which requires planes with the least possible distortion. This can best be satisfied by the most homogeneous distribution of stacking faults in the fcc lattice, but not by a hex. lattice²⁾.

Summary

- 1) Martensitic single crystals of ternary CuZnAl show a stress induced transformation from the martensitic 3R to an fcc ordered structure. The corresponding critical resolved shear stress τ_B is very weakly dependent on temperature but is strongly affected by the alloy composition. The τ_B has been measured for alloys with the same M_s temperature but different electron concentration e/a and for alloys with constant e/a but varying M_s .
- 2) The results are analysed in terms of a contribution that depends on order, i.e. on the distribution of the atoms, and another that is a function only of the electron concentration.
- 3) It is shown that the order contribution is controlled by the chemical interaction energies between fourth nearest neighbors. Numerical values are calculated, which are in excellent agreement with those obtained from the analysis of the M_s temperature.
- 4) By subtracting the order contribution, the energy difference between the hypothetical disordered 3R and fcc structures has been calculated. It is shown that it is related to the stacking fault energies in the α phase solid solution range, and that the regularity of the stacking fault distribution in martensite does not constitute an additional element of phase stabilisation.
- 5) It is concluded that the 3R martensite in the CuZn alloys is less stable than a hex. martensitic phase, but that its formation is related to the mechanism of the martensitic transformation, which requires an undistorted habit plane.

This work was partially supported by the Argentinian Consejo Nacional de Investigaciones Científicas y Técnicas, Código 01 AB2 - 05-008. Discussions and a critical reading of the manuscript by Dr. M. Chandrasekaran is gratefully acknowledged.

Literature

- 1) W. ARNEODO and M. AHLERS, *Scripta Met* **7** (1973) 1287.
- 2) W. ARNEODO and M. AHLERS, *Acta Met* **22** (1974) 1475.
- 3) R. RAPACIOLI and M. AHLERS, *Acta Met*, to be published.
- 4) C. S. BARRETT and T. B. MASSALSKI, *Structure of Metals*, McGraw Hill, New York 1966.
- 5) G. INDEN, *Z. Metallkde.* **66** (1975) 648.
- 6) G. INDEN, *Z. Metallkde.* **66** (1975) 577.
- 7) M. AHLERS, *Z. Metallkde.* **70** (1979) 379.
- 8) S. W. WILKINS and C. G. SHIRLEY, *J. Appl. Cryst.* **8** (1975) 107.
- 9) J. FRIEDEL, *Nuovo Cim. (Suppl)* **7** (1958) 287.
- 10) R. RAPACIOLI and M. AHLERS, *Scripta Met.* **11** (1977) 1147.
- 11) L. DELAEY, *Z. Metallkde.* **58** (1967) 389.
- 12) M. AHLERS, *Scripta Met.* **8** (1974) 213.
- 13) H. POPS and N. RIDLEY, *Met. Trans.* **1** (1970) 2653.
- 14) P. HAASEN, *Suppl. Trans. Jap. Inst. Me.* **9** (1968) 40.
- 15) P. C. J. GALLAGHER, *Met. Trans.* **1** (1970) 2429.
- 16) C. B. CARTER and I. L. F. RAY, *Phil. Mag.* **35** (1977) 189.
- 17) L. REMY, A. PINEAU, and B. THOMAS, *Mat. Sci. Eng.* **36** (1978) 47.

(Eingegangen am 10. April 1979)